2021

Experimental Investigation On Organic Rankine Cycle In Off-Design Conditions

Jinwoo Oh
Korea University, Korea, Republic of (South Korea), squuuidoh@korea.ac.kr

Hoyoung Jeong

Hoseong Lee

Experimental Investigation on Organic Rankine Cycle in Off-Design Conditions

Jinwoo Oh[1], Hoyoung Jeong[1], Hoseong Lee[1]*

[1]Korea University, Department of Mechanical Engineering,
Seoul, Anam-Dong, Seongbuk-Gu, Republic of Korea
Contact Information (hslee1@korea.ac.kr)

* Corresponding Author

ABSTRACT

An experimental study is conducted to investigate the thermal-hydraulic characteristics of organic Rankine cycle in off-design conditions using R245fa as the working fluid. The effects of off-design conditions are monitored by varying the boundary conditions of the system in a total of 97 data sets. The charge distribution in the system is examined by applying the density-volume-measurement method in each component while the void fraction model is used for the prediction of captivated mass inside the heat exchangers. The simulation results of the heat exchanger models were validated with the experimental results within 5% error range. The working fluid charge ratio is varied between 30~70% in both basic and recuperative cycle configuration. A passive-design is proposed to determine the liquid level of the liquid receiver in the perspective of mass conservation. The impact of fluid over-charge and under-charge phenomena are thoroughly examined which result in system failure. The heat source and sink operating conditions are varied in order to observe the part-load response of the system. The results indicate that there exists a significant disadvantage when applying the recuperator in the cycle. Dominant factors that determine the evaporation and condensation pressure are discussed in terms of charge distribution.

1. INTRODUCTION

The shift in the phase of energy policy has created a need for a variety of facilities capable of handling local energy demand through dissipation of heat and power supply. As part of the transition, much attention is being paid to the organic Rankine cycle (ORC), which can generate effective power from renewable energy sources and industrial waste heat. However, due to the fluctuating nature of these resources, unintended system operation has deviated from its nominal point, and this is called off-design operation. Numerous studies have been carried out by changing the system boundary conditions in various aspects to investigate system performance under off-design conditions. Nevertheless, consideration of the impact of system charge has often been neglected, and the importance of that analysis has only recently been emphasized.

The first study of the effect of fluid charge on ORC performance was described by Li *et al.* (2015). The authors defined a dimensionless parameter of the volume ratio to find the optimal filling conditions for the cycle. Kim *et al.* (2017) also changed the amount of mass in the system at low temperatures below 80°C. The output of the expander was observed to be highest at a charge rate of 32.6%. Later, Liu *et al.* (2019) investigated the effects of overcharging and undercharging on the system and explained that both reduce the isentropic efficiency of the expander for a specific shaft torque. In addition, when the filling amount was insufficient, the mass flow rate was found to be unstable due to cavitation of the pump. The change in liquid level in the working fluid tank was determined by Cao *et al.* (2019), who measured the liquid level using a magnetic float on the outer tube connected to the tank. Dickes *et al.* (2020) implemented an online measurement method for mass distribution monitoring, unlike previous studies that only measured the total charged mass, and measured the weight of major parts in real time.

Throughout the literature review, it can be seen that research regarding the charged mass is still in infancy stage and only superficial results were derived from the previous studies. In this study, the underlying mechanisms of low-temperature heat recovery ORC operating under off-design conditions are intensively investigated by experimental research with the aid of numerical models. Experiments were conducted on a 1 kW lab-scale ORC testbed using R245fa as the working fluid. The effect of four key operating conditions on system performance, including charged mass, is thoroughly investigated. Numerical models of the heat exchangers are developed and validated based on the tested data to support the interpretation of the experimental results. The performance of the basic and recuperative

ORC is evaluated and compared to each other to analyze the effect of recuperator heat recovery. The process of formation of the evaporation and condensation pressures is revealed in terms of controllability and mass balance. The liquid level in a liquid receiver is predicted analytically that cannot be understood by conventional thermodynamics. The change in mass distribution is evaluated and the effect of liquid holdup in the heat exchangers is visualized through the simulation results.

2. Experiment

2.1 ORC system

The photograph of the 1 kW lab-scale ORC testbed is shown in Figure 1. R245fa is selected as the working fluid and water is used as the heat sink and source fluid. The heat sink water is cooled and circulated by the air-cooled chiller, and the heat source water is heated and pressurized by the electric heater. The heat capacity of the air-cooled chiller and electric heater is 25 kW and 21 kW, respectively. The ORC unit consists of five main components: pump, evaporator, condenser, expander and liquid receiver. A six-pole asynchronous motor connected to the pump reciprocates the diaphragm to pressurize the working fluid and deliver it to the evaporator. Brazed plate heat exchangers are used for the evaporator and condenser. The oil-free scroll expander is located between the high- and low-pressure sides of the system which generates power. In order to measure the shaft torque and rotational speed of the expander, the device was modified from semi-hermetic to open-drive type expander. Finally, the liquid receiver is used as a buffer located between the condenser and the diaphragm pump, so that only liquid is supplied to the pump.

Figure 1: Photograph of the 1 kW lab-scale ORC testbed

2.2 Test procedure

The operating conditions of the experimental study are summarized in Table 1. Parametric studies were conducted by independently changing the boundary conditions of the ORC system. In this study, three test matrices were performed to observe the effects of charged mass, heat sink temperature, and expander rotation speed under low temperature heat source conditions. The first test matrix was conducted by charging the system with an increment of 0.5 kg in each set of experiments. The second test matrix was carried out by changing the setting temperature of the air-cooled chiller in order to reflect the daily or interseason change in ambient temperature. Lastly, the third test matrix was executed by varying the expander rotational speed by using a variable frequency drive connected to the generator. The heat source temperature increased from 65°C to 95°C in 10°C increments for all test matrices.

Table 1: Test matrices of the experimental study

Test matrix	Parameter	Value	Step size	Unit
1	Charged mass	3.5-7.5	0.5	kg
	Heat source temperature	65-95	10	℃
2	Heat sink temperature	8-24	4	℃
	Heat source temperature	65-95	10	℃
3	Expander rotational speed	1,600-3,000	350	rpm
	Heat source temperature	65-95	10	℃

3. Numerical models

3.1 Internal mass

The internal volume of each component was obtained through a three-dimensional computer-aided design and direct measurement of the geometry, as shown in Table 2. Since the average density of the single-phase components can be obtained, the internal mass of the single-phase components is calculated using the density-volume measurement method as Equation (1).

$$M_{sp} = \bar{\rho}_{sp} V_{sp} \tag{1}$$

Nonetheless, in the case of the phase-changing components, evaporator and condenser, the captured mass cannot be predicted by only using Equation (1). As a result, the two-phase mass needs another consideration by applying the void fractions as noted in Equation (2).

$$M_{tp} = M_l + M_v = A_c \left[\rho_l \int_0^L (1-\alpha)\, dl + \rho_v \int_0^L \alpha\, dl \right] \tag{2}$$

The charged mass inside the system is distributed in every component that compose the ORC. In steady-state operation, the amount of internal mass captured by each component is fixed and the summation of the mass should equal the total charged mass according to the law of mass conservation as seen in Equation (3).

$$M_{ch} = M_{pp} + M_{ev} + M_{ex} + M_{cd} + M_{lr} + M_{rec} + M_{pipe} + M_{dev} \tag{3}$$

Table 2: Internal volume of the components of the ORC

Location	Volume (cm^3)
Pump	20.0
$Recuperator_l$	238.3
Evaporator	2206.6
Expander	334.0
$Recuperator_v$	294.4
Condenser	1485.9
Liquid receiver	3011.3
Measurement devices	87.6

3.2 Heat exchangers

Unlike other components, the working fluid experiences a phase change inside the evaporator and condenser, causing problems when evaluating the internal mass of the instrument. Therefore, iterative numerical models are used for the

intensive analysis of the of heat exchangers. The flow chart of the heat exchanger model is illustrated in Figure 2. The heat exchanger model was developed by Jeong *et al.* (2020) by utilizing a discretization method in which the heat exchanger is evenly divided into n segments in the flow direction. In all cases, the flow direction is counterflow and the input parameters are inlet temperature, pressure, and mass flow rate for both fluids X and Y. Here, the phase of fluid X undergoes a phase change during heat transfer and fluid Y remains the same. Because heat transfer occurs at the plate surface, the simulation is initiated by assuming guess values for the exit condition of fluid Y at node number i=0. The Nusselt number and friction factor are then calculated according to the thermal conditions of the two fluids. The thermal condition of the following node i+1 is derived through the effectiveness-NTU method and pressure drop analysis. After successive calculations, the convergence is confirmed by comparing the simulation and experimental results of the fluid Y inlet temperature. Finally, the simulation process ends when the convergence criterion is met, otherwise it starts again with a new guess. The output parameters are the outlet temperature and pressure of both fluids, the total heat transfer rate, and the mass of fluid X.

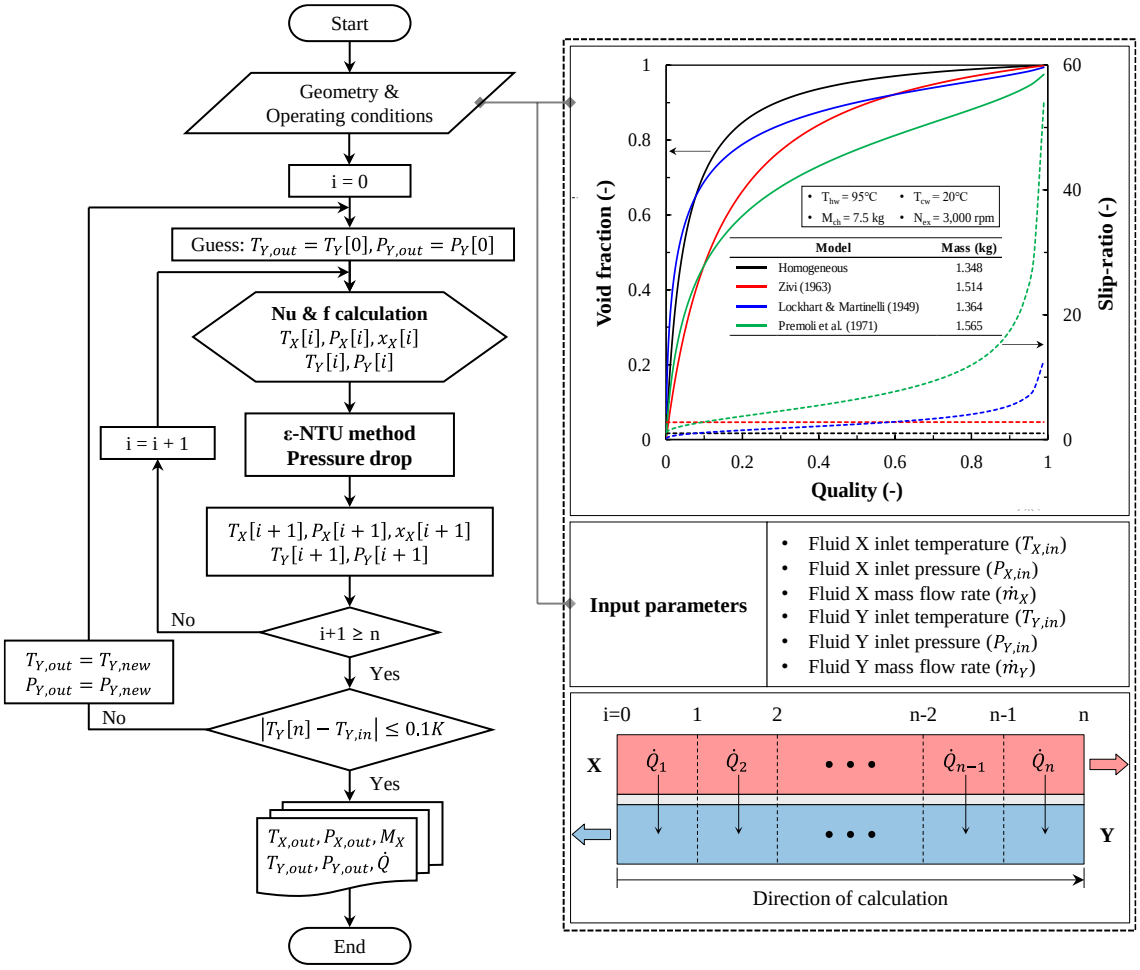

Figure 2: Flowchart of the heat exchanger model

4. Results

4.1 Validation of heat exchanger model

The simulation results of the numerical model are compared with the experimental results of 97 data sets. Mean absolute percent error (MAPE) and relative mean squared error (RRMSE) are evaluated on each parity plot. The comparison of the heat transfer rate and outlet pressure of the heat exchanger is shown in Figure 3 (a) and (b). The heat transfer rate and outlet pressure are predicted within 1.6% and 5.5% error ranges, respectively. Thus, the numerical model is very accurate and suitable for in-depth analysis of system characteristics.

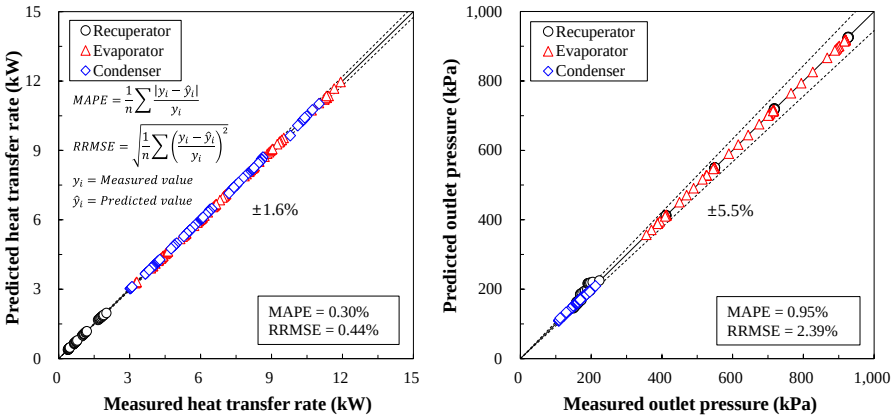

(a) Comparison of heat transfer rate (b) Comparison of outlet pressure

Figure 3: Validation results of the heat exchanger model

4.2 System performance investigation

4.2.1 Effect of boundary condition variation: The test results of the three test matrices in section 2.2 are depicted in Figure 4. The effect of charged mass variation on the system performance and T-s diagram is shown in Figure 4 (a). The system did not work when the charged mass was less than 3.5 kg or more than 7.5 kg in all heat source temperature ranges. The electrical efficiency tends to decrease as the charged mass increases, where this relationship means that the condensation pressure is influenced by the charged mass, since the high-pressure side of the system was kept constant in all cases. This change in condensation pressure can be observed in the T-s diagram as the pressure ratio decreases as the charged mass increases.

The impact of heat sink temperature variation on the system performance and T-s diagram is shown in Figure 4 (b). Similar to the results of the charged mass variation, the condensation pressure increases as the heat sink temperature increases, resulting in the decrease of the pressure ratio. As a result, the electrical efficiency decreases, while the high-pressure is nearly unaffected by the increase in heat sink temperature.

The influence of expander rotational speed variation on the system performance and T-s diagram is shown in Figure 4 (c). Unlike the previous results, the electrical efficiency tends to show different trends depending on the rotational speed. This is because the expander volumetric efficiency is dependent on the rotational speed, which affect the amount of mass leakage as described by Oh *et al.* (2020). In addition, since the mass flow rate is kept constant, only the high-pressure decreases as the rotational speed increase owing to the decrease in flow resistance.

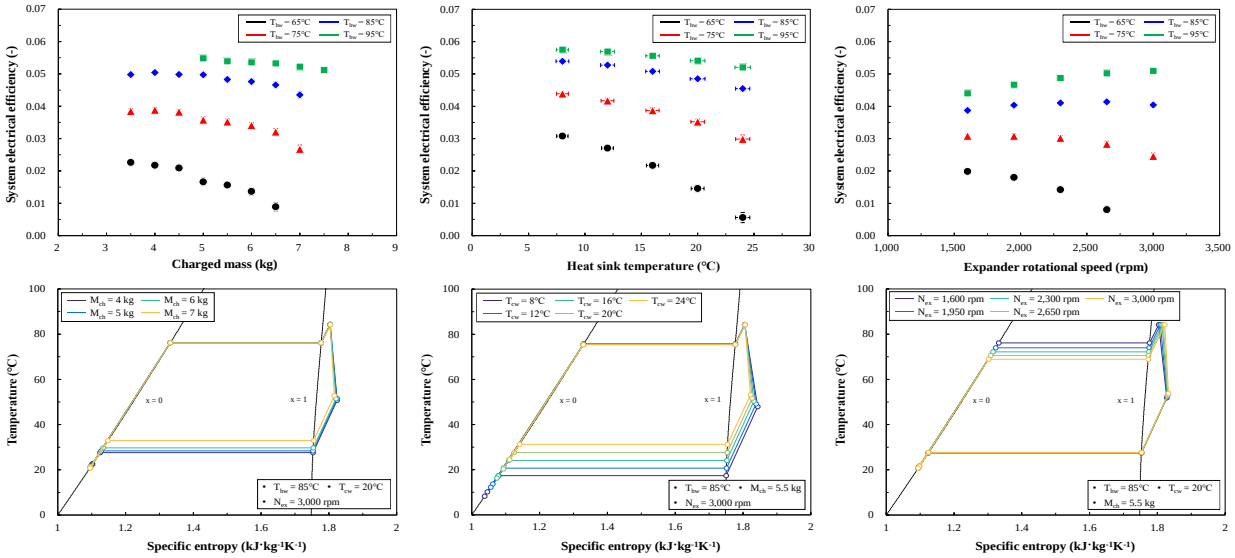

(a) Effect of charged mass variation (b) Effect of heat sink temperature variation (c) Effect of expander rotational speed variation

Figure 4: Influence of various boundary conditions on the system performance and T-s diagram

4.2.2 Comparison of basic and recuperative ORC: The performance comparison and investigation on basic ORC (BORC) and recuperative ORC (RORC) are illustrated in Figure 5. The evaporator heat transfer rate and expander shaft power of the BORC and RORC are indicated by the filled and unfilled markers, respectively, and can be seen in Figure 5 (a) and (b). The evaporator heat transfer rate of the RORC was decreased by an average of 13% compared to that of the BORC, which indicates that the internal heat recovery effect of the recuperator is evident. Nevertheless, the expander shaft power was also reduced by an average of 24.6%, resulting in an overall reduction in system efficiency by 17.6%.

This unexpected degradation of the system efficiency and generated power originated from the recuperator itself as seen in Figure 5 (c) and (d). The linear relationship between the shaft torque and expander pressure difference infers that the recuperator raised the outlet pressure of the expander, since the inlet pressure was kept constant. This is because the vapor-side recuperator behaves as a flow resistance while the working fluid is high in velocity after the expansion process. The specific values of the pressure drop in various locations are shown in Figure 5 (d). The pipe pressure drops of the BORC and RORC are comparatively similar to each other, considering the extended pipe length for the recuperator connection. However, the vapor-side recuperator pressure drop appeared to be approximately twice the pipe pressure drop. In conclusion, the test results inform that the impact of power loss can be greater than that of the heat gain when using a recuperator, which deteriorates the overall performance of the RORC. It is noteworthy that the outlet pressure of the expander always increases with the use of recuperator regardless of the type of heat exchanger. Furthermore, in applications where waste heat is recovered by ORC, discussing the system efficiency is pointless because there is no heat investment into the system. In all circumstances, the BORC is always superior to RORC in terms of power generation.

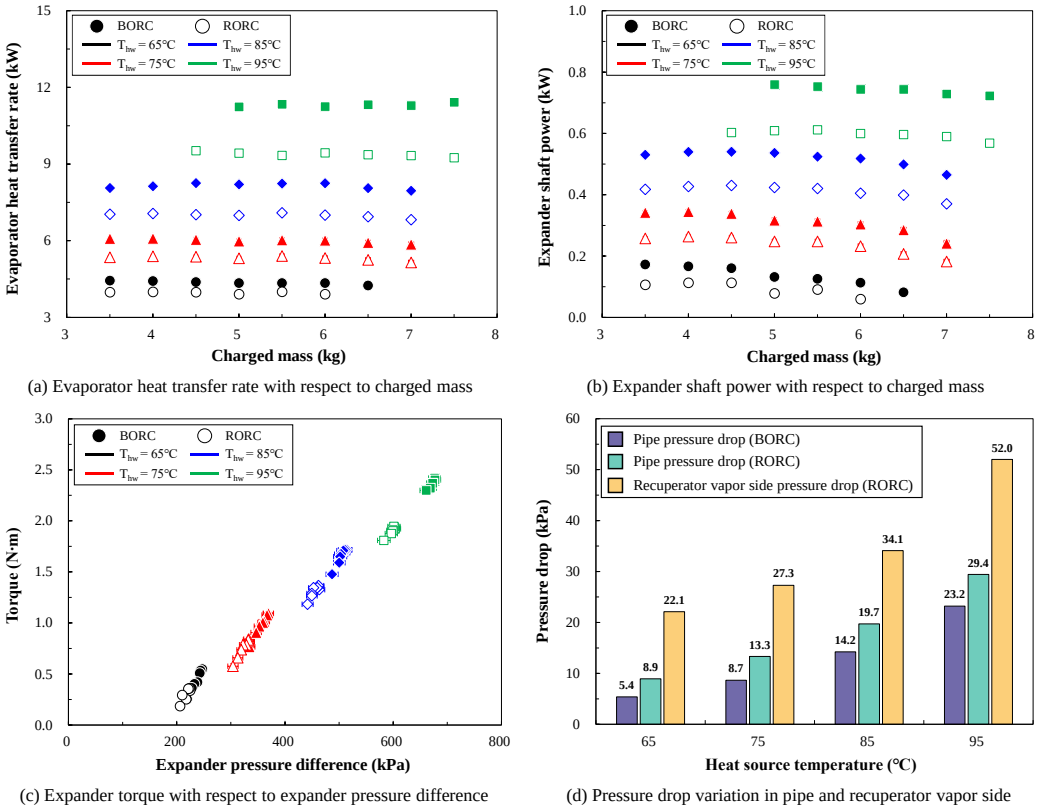

(a) Evaporator heat transfer rate with respect to charged mass

(b) Expander shaft power with respect to charged mass

(c) Expander torque with respect to expander pressure difference

(d) Pressure drop variation in pipe and recuperator vapor side

Figure 5: Performance comparison and investigation on BORC and RORC

4.3 High- and low-pressure formation process

The high- and low-pressure characteristics of the ORC system are shown in Figure 6. The condensation and evaporation pressures are indicated by filled and unfilled markers, respectively, as shown in Figure 6 (a). During the experiment, the evaporation pressure was controlled by changing the rotational speed of the pump and expander. The relative rotational speed of the rotating equipment can be reflected by introducing the volumetric flow rate ratio as seen in Equation (4).

$$r_{\dot{V}} = \frac{\dot{V}_{ex}}{\dot{V}_{pp}} = \frac{\rho_{pp}}{\rho_{ex}} \tag{4}$$

The evaporation pressure increases as the volumetric flow rate ratio decreases. This is because the high-pressure builds up proportionally as the flow resistance increases. In other words, the decrease in pump rotational speed or increase in expander rotational speed, results in the decrease in evaporation pressure. This means that the evaporation pressure can be controlled by adjusting the operating conditions of the rotating device. On the other hand, the condensation pressure cannot be controlled and is determined by other operating conditions such as the charged mass and heat sink conditions.

This feature is evident as seen in Figure 6 (b), where the condensation pressure is plotted against the liquid level of the liquid receiver. As the charged mass increases, the condensation pressure increases as well as the liquid level. When the liquid level is below the liquid receiver outlet, the system is undercharged and the pump fails to operate due to insufficient subcooling. Meanwhile, when the liquid level becomes equal to the maximum height of the liquid tank, the system is overcharged and the expander fails to operate owing to the sharp increase in the condensation pressure.

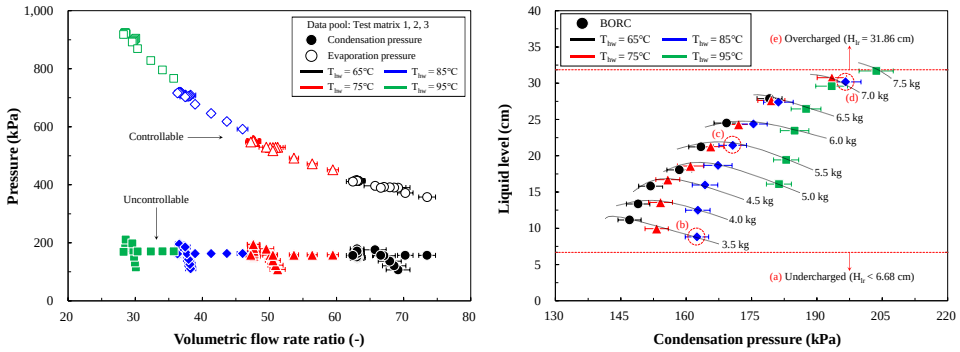

(a) High- and low-pressure with respect to volumetric flow rate ratio (b) Liquid level variation of the liquid receiver

Figure 6: Performance comparison and investigation on BORC and RORC

4.4 Liquid holdup effect of heat exchangers

The three main components that capture the charged mass are the evaporator, condenser and liquid receiver. Other components include pump, expander, pipelines, recuperator, and measuring devices grouped together. The mass inside the pump and expander, respectively, is negligible due to its small volume and low density. The mass required for the evaporation line depends entirely on the heat source and working fluid conditions, whereas that of the condensation line is simply the residue that has not been consumed by the high-pressure side.

The effect of heat source temperature change on the mass distribution is shown in Figure 7 (a) and (b). When the heat source temperature rises, more mass accumulates inside the evaporator because an increase in mass flow rate and evaporation pressure delays the evaporation of the working fluid. As a result, the proportion of supercooled liquid in the evaporator increases, increasing the distribution ratio. On the other hand, the increase in the heat source temperature also delays the condensation of the working fluid inside the condenser, resulting in a reduction in the supercooled liquid surrounded by the condenser. As a result, the liquid holdup effect of the heat exchangers dominates the mass distribution of the ORC and the trade-off relationship for mass between heat exchangers can be observed.

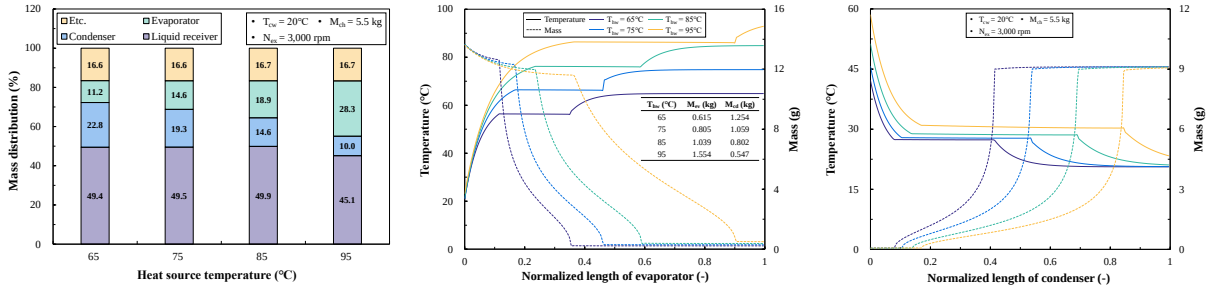

(a) Mass distribution ratio according to heat source temperature (b) Temperature and mass profile of the evaporator and condenser

Figure 7: Liquid holdup effect of heat exchangers on the mass distribution

5. CONCLUSIONS

In this study, the empirical and theoretical methods are used to understand the principle of thermal-hydraulic behavior of low-temperature off-design ORC systems. Experiments have been carried out and the simulation results of the heat exchangers are verified based on the tested data. Analysis dealing with the effects of recuperative heat recovery, pressure build-up processes and liquid level yielded unprecedented results. Notable conclusions are summarized as follows:

- The effect of the four boundary conditions on the system performance is investigated through experimental parametric studies. Increasing the charged mass and heat sink temperature reduced the overall performance, but the increase in the expander rotation speed led to different trends due to the effect of the expander volumetric efficiency.
- Contrary to common belief, the performance of RORC was 17.6% lower than that of BORC, despite the use of recuperator because the expander performance was degraded due to excessive pressure drop. Proper design of the recuperator can increase the efficiency of RORC, but cannot be larger in terms of power generation compared to BORC.
- The evaporation pressure is controllable and can be predicted by evaluating the volumetric flow rate. On the other hand, the condensation pressure is uncontrollable.
- The system may be undercharged or overcharged depending on the operating conditions and the size of the entire system and liquid receiver. The system will not work in undercharged or overcharged situations due to pump or expander failure, respectively.
- The mass distribution of the charged mass is mainly determined by the liquid holdup effect of the evaporator and condenser.

NOMENCLATURE

A_c	cross-sectional area	(m^2)
α	void fraction	(–)
M	mass	(kg)
$r_{\dot{V}}$	volumetric flow rate ratio	(–)
ρ	density	(kg/m^3)
V	volume	(m^3)
$\dot{V}$	volumetric flow rate	(m^3/s)

Subscript

cd	condenser
ch	charged
ev	evaporator
ex	expander
l	liquid
lr	liquid receiver
pp	pump
rec	recuperator
sp	single phase
tp	two phase
v	vapor

REFERENCES

Cao, S., Miao, Z., & Xu, J. (2019). The effect of liquid charge ratio on organic Rankine cycle operation. *Applied Thermal Engineering*, *162*, 114227.

Dickes, R., Dumont, O., & Lemort, V. (2020). Experimental assessment of the fluid charge distribution in an organic Rankine cycle (ORC) power system. *Applied Thermal Engineering*, *179*, 115689.

Jeong, H., Oh, J., & Lee, H. (2020). Experimental investigation of performance of plate heat exchanger as organic Rankine cycle evaporator. *International Journal of Heat and Mass Transfer*, *159*, 120158.

Kim, D. K., Lee, J. S., Kim, J., Kim, M. S., & Kim, M. S. (2017). Parametric study and performance evaluation of an organic Rankine cycle (ORC) system using low-grade heat at temperatures below 80 C. *Applied energy*, *189*, 55-65.

Li, T., Zhu, J., Fu, W., & Hu, K. (2015). Experimental comparison of R245fa and R245fa/R601a for organic Rankine cycle using scroll expander. *International Journal of Energy Research*, *39*(2), 202-214.

Liu, L., Zhu, T., Wang, T., & Gao, N. (2019). Experimental investigation on the effect of working fluid charge in a small-scale Organic Rankine Cycle under off-design conditions. *Energy*, *174*, 664-677.

Oh, J., Jeong, H., Kim, J., & Lee, H. (2020). Numerical and experimental investigation on thermal-hydraulic characteristics of a scroll expander for organic Rankine cycle. *Applied Energy*, *278*, 115672.

ACKNOWLEDGEMENT

This research was supported by the Energy Efficiency & Resources Core Technology Program of the Korea Institute of Energy Technology Evaluation and Planning (KETEP), funded by the Ministry of Trade, Industry & Energy, Republic of Korea. (No. 2018201060010B).